

1 **Modifying drug release for intramuscular and oral delivery using drug-eluting**
2 **embolisation beads**

3

4 **Abstract**

5 In recent years, polymer-based embolisation beads have been used to deliver drugs for the treatment
6 of cancer directly to the site of action. Known to be biocompatible implants, these beads have become
7 an ideal drug delivery vehicle for parenteral administration yet have not been considered for the more
8 commonly used drug delivery routes such as oral and intramuscular drug delivery. This work
9 describes the application of a type of polymer beads, formerly used for embolisation, as a formulation
10 option for oral and intramuscular delivery of a model drug, namely imipramine. Following successful
11 incorporation within the beads, dissolution analysis confirmed the potential to provide a modified
12 drug release profile. Thermogravimetric analysis (TGA) permitted determination of the total water
13 content within the beads (96.8 %) and differential scanning calorimetry (DSC) indicated that not all of
14 the water within the beads was able to freeze, apportioned as 15.8 % non-freezing, 25.1 % loosely
15 bound and the remaining 55.9 % unbound. In the presence of drug, the size of the beads decreased
16 with a reduced water content (95.4 %) comprised of 16.7 % non-freezing, 20.5 % freezing bound and
17 the remaining 58.2 % unbound. In conclusion, the results presented in this study confirm the ability
18 of TGA and DSC to separate the differing types of water within the beads and furthermore, the
19 potential of such beads for a far wider variety of formulation options than those previously adopted.

20 **Keywords:** beads; drug-eluting; DSC; intramuscular; modified; polymer.

21

22

23

24

25

26

27

28

29 **Introduction**

30 Although oral delivery of drugs is by far the simplest, cheapest and most desirable route of
31 administration, it is sometimes not possible to formulate in a manner that would ensure a suitable

32 level of bioavailability can be attained. In such cases it is sometimes necessary to create a modified-
33 release formulation that exhibits a drug release profile that facilitates a suitable rate and extent of drug
34 release for patient optimisation. Several strategies to modify drug release have been developed over
35 the years including gelatin/non-gelatin capsules (Gullapalli and Mazzitelli, 2017), mesoporous silica
36 materials (Maleki et al., 2017; Waters et al., 2018), liposomes/niosomes (Manna et al., 2019), inclusion
37 complexes (such as cyclodextrins (Budai-Szucs et al., 2018), polymers (Wersig et al., 2018) and many
38 others such as nanocarriers (Dey et al., 2019; Cai et al., 2023). Such formulations have successfully
39 created a wide variety of drug release profiles with a range of positive impacts such as reducing
40 dosing intervals or side effects, in some cases increasing bioavailability and generally increasing
41 patient compliance. However, even with the strategies previously considered, some drugs continue to
42 present a formulation issue and still require the development of a suitable modified release
43 formulation to enhance their drug release profiles (Boon-in and Crespy, 2023). One such drug is
44 imipramine hydrochloride, a tricyclic antidepressant, with a wide bioavailability range from 22 to
45 77% (Ramey et al., 2014; Oliver et al., 2022), time to peak drug level of three hours (Abernethy et al.,
46 1984) and known age-dependent rate of clearance (Abernethy et al., 1985). The drug is used in the
47 treatment of depression and anxiety, administered either through intramuscular or oral delivery, the
48 former usually for short term dosing and the latter for the longer term. With variable bioavailability
49 both options exhibit far from ideal drug release profiles and ideally an alternative formulation option
50 could be developed that delivers a constant and stable plasma concentration to avoid highly variable
51 pharmacokinetic characteristics (Ullmann et al., 2001) also, one which is more suited to the rapidly
52 increasing elderly population (Khan and Roberts, 2018). One group of potential formulation enhancers
53 that have not previously been considered for such a purpose are the well-characterised, drug-eluting
54 embolisation beads, currently used in the treatment of liver cancer whereby a drug/device
55 combination is created based on a microspherical polymer bead, such as DC Bead LUMI™ (Caine et
56 al., 2018; Lewis et al., 2018) or DC Bead MI™ (Lewis et al., 2016). Drugs including doxorubicin are
57 bound to the structure of the bead prior to administration with intended release at the site of
58 action (Xie et al., 2023). Previous work from our group has utilised isothermal titration calorimetry to
59 measure the binding interaction of such drug based systems and determined the drug to binding sites on
60 the bead ratio where the intended application is transarterial chemoembolisation (Swaine et al., 2019;
61 Waters et al., 2015). However, these drug-eluting beads (DEBs) have only been considered for this
62 specific purpose yet could hold great promise as a simple yet effective method of modified drug
63 release for use in intramuscular and oral delivery for a wide range of drugs, in this case, for
64 imipramine hydrochloride as a model compound.

65

66 **Materials and Methods**

67 **Materials**

68 Polymer beads (70-150 µm (DC BeadMI™) were kindly donated by Biocompatibles UK Ltd., a BTG
69 International group company (Camberley, UK). Imipramine hydrochloride (>99%) was purchased from
70 Tokyo Chemical Industry Ltd. (Oxford, UK). Potassium phosphate dibasic and potassium phosphate
71 monobasic (both ≥ 99 %) were purchased from Sigma Aldrich (Dorset, UK) and used as received. De-
72 ionised water was used throughout the experiments.

73
74 **Methods**

75 **Imipramine loading into beads**

76 1 mL of DC BeadMI™ was transferred into a vial using a measuring cylinder and the majority of the
77 packing salt solution removed with a pipette to leave a slurry of beads. Imipramine hydrochloride
78 solution (10 mg/mL) was added with a volume of 1 mL, 2.5 mL, and 5 mL to target 10, 25, and 50 mg
79 loadings, respectively, followed by occasional gentle agitation and left overnight. The residual
80 solution was diluted and the UV absorbance was measured using UV-Vis spectrophotometry at 250
81 nm and compared with a standard plot to determine the amount of drug remaining in solution (and
82 hence by subtraction that loaded into the beads).

83
84 **Optical microscopy, bead sizing and water content estimation**

85 Optical microscopy and measurement of bead sizes were carried out using a BX50 microscope and a
86 10x dry objective. (Olympus UK Ltd, Essex, England). The eyepiece graticule used to measure the
87 beads was verified using a calibrated graticule placed on the microscope stage (Graticules Ltd, Kent,
88 England). A monolayer of bead sample was placed in a Petri dish on the microscope stage and using
89 the 10x objective and eyepiece graticule, the diameter of 200 individual beads was measured. The
90 bead sizing data was entered into a spreadsheet and the size histograms generated using Prism 6
91 (GraphPad Software, Inc., La Jolla, CA). Based on the size change of beads and the assumption that
92 size decrease is a consequence of water displaced from beads by the drug, the water content in drug
93 loaded beads was calculated as follows:

94
$$\text{Water content} = \frac{\text{Volume of water in bland beads} - \text{Volume of water loss after drug loading}}{\text{Volume of drug loaded beads}} \times 100\%$$

95
96 In the calculation, Volume of water loss after drug loading = Volume of bland beads – Volume of
97 drug loaded beads.

98
99 **Dissolution studies**

100 Drug release testing was carried out by using the USP Type II Method. The drug loaded beads were
101 first washed with 5 mL of deionised water, then were added into 200 mL of pH 7.0 PBS at 37 °C
102 under constant magnetic stirring. At predetermined time points, 5 mL of solution was withdrawn
103 through a 5 µm filter needle, and 5 mL of fresh PBS was added. The solution was measured by UV
104 spectrophotometry at 250 nm to calculate the drug concentration released. Samples were analysed in
105 triplicate to determine mean drug release percentages and associated error limits. Dissolution profiles
106 were compared with those already published for other drugs alongside imipramine, to allow
107 comparisons with other controlled release formulations.

108

109 **Thermogravimetric analysis(TGA)**

110 A Mettler Toledo (TGA) was used to investigate the total water content of the beads. Samples were
111 filtered to remove excess water, ranging from 4 – 16 mg, were placed on an aluminium holder and
112 heated from 25 to 120 °C with a nitrogen carrier gas flow of 80 mL/min and heating rate of 1 °C/min.
113 Weight loss as a function of temperature change was recorded with the total loss equated to the water
114 content within the beads (n=3 per heating rate) both with and without the presence of drug.

115

116 **Differential scanning calorimetry (DSC)**

117 Differential scanning calorimetry (DSC) was performed using a Mettler Toledo DSC 1 equipped with
118 chiller cooling apparatus. Samples (filtered to remove excess water)of water, beads and drug with
119 beads ranging from 4 to 10 mg in sealed aluminium pans were heated at a rate of 1°C/minunder a
120 nitrogen flow of 80 mL/min from -20 to 20 °C (n=3 per heating rate). Using this data it was possible
121 to quantify the amount of water within the beads that was able to undergo the freezing process, i.e.
122 was not tightly bound to the polymer structure. This was based on the assumption that ‘bound’ water
123 would not contribute to the peak observed within the DSC profile thus subtracting the water
124 associated with the peak observed with DSC from the total water content observed from TGA allowed
125 calculation of the amount of ‘unbound’ water within the beads.

126

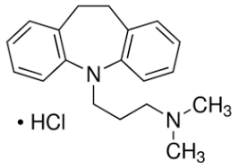
127 **Results and Discussion**

128 **Drug loading evaluations**

129 Beads containing the model drug were formulated and then analysed as described in the Methods
130 section. Drug loading studies permitted calculation of the amount of imipramine hydrochloride loaded
131 per mL of hydrated beads from the three different drug concentration solutions (Table 1).For the 10
132 mgmL⁻¹, 25 mgmL⁻¹ and 50 mgmL⁻¹drug concentrations, beads were found to load95.2%, 92.5% and
133 61.5% of the drug respectively. Drug interaction is presumed to be *via*an ion exchange process as for
134 other reported hydrochloride salts (Lewis, 2009)through the tertiary amine group pendent to the ring

135 structure. At lower concentrations (10 & 25 mg), loading efficiency was relatively high (>90%) as the
 136 number of cationically-charged binding groups on the drug was less than the number of anionic
 137 sulfonate groups in the bead structure. For the 50 mgmL⁻¹ loading, the number of drug binding groups
 138 is in excess and loading is saturated at 62% loading, where all binding sites are occupied by drug
 139 molecules. This equates to around 30 mgmL⁻¹ maximum loading potential for imipramine
 140 hydrochloride.

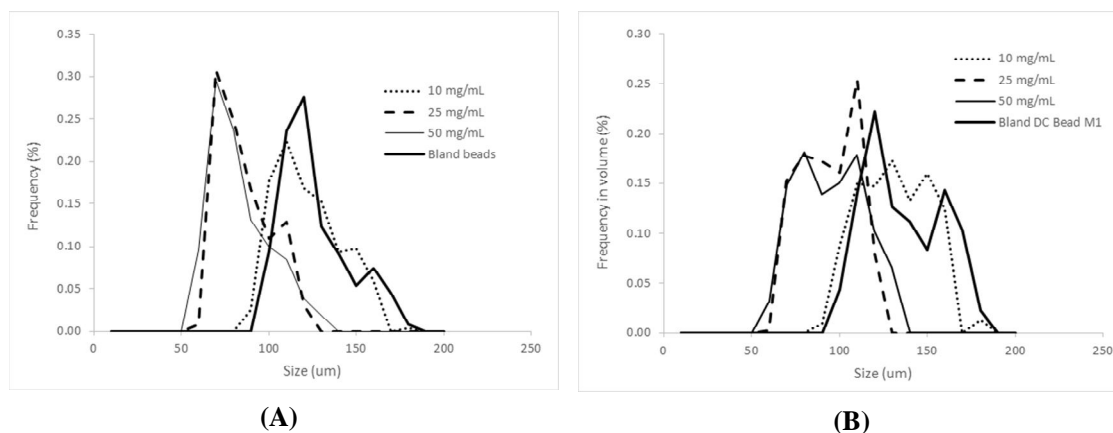
141 Table 1: Drug structure and loading amount and efficiency in 1 mL of DC Bead *MI* (n=3)

	Target loading (mgmL ⁻¹)	Loading (mgmL ⁻¹)	Loading yield (%)
	10	9.52 ± 0.01	95.19 ± 0.09
	25	23.13 ± 0.27	92.54 ± 1.09
	50	30.76 ± 2.65	61.53 ± 5.29

142

143 Optical microscopy analysis of the beads indicated that their average size decreased when drug
 144 loading was greater than 10 mgmL⁻¹ (Figure 1 and 2), with the greatest change seen from 121 ± 19 μm
 145 to 79 ± 17 μm following loading with the highest concentration of drug (see Table 1). This is
 146 consistent with what has been observed previously with other cationically-charged drugs, where bulky
 147 drugs with hydrophobic components enter the hydrogel matrix and bind to the anionic sulfonate
 148 moieties, resulting in water being displaced from the interstitial spaces between polymer chains,
 149 decreasing the water content and causing the beads to shrink in diameter (Lewis et al., 2006; Taylor et
 150 al., 2007).

151



152 Figure 1: Size (A) and volume (B) distribution of bland DC Bead *MI*, 10 mgmL⁻¹, 25 mgmL⁻¹, and
 153 mgmL⁻¹ drug loaded beads.

154

155

156 Table 2: Data for bead sizes and estimated water fraction in beads

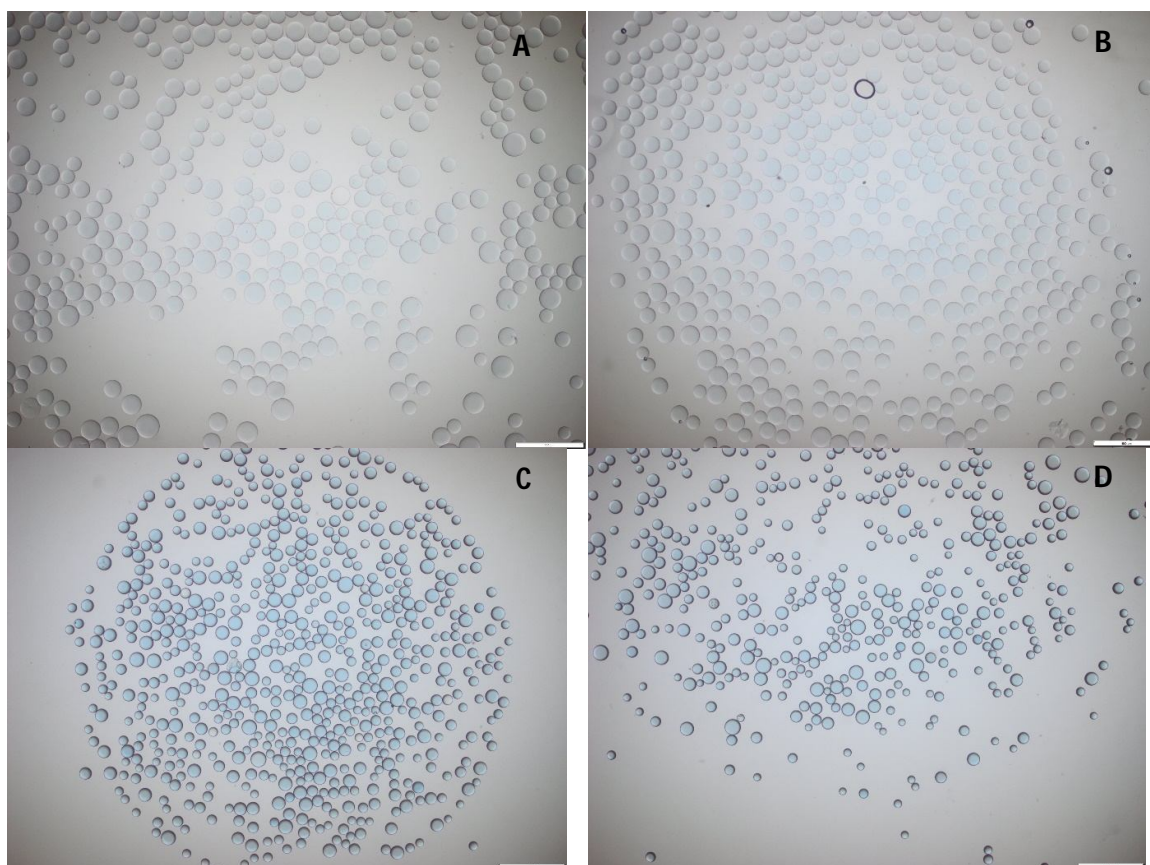
	Bland	10 mgmL ⁻¹	25 mgmL ⁻¹	50 mgmL ⁻¹
Bead size range (µm)	91.1-175.5	84.4-178.9	57.4-118.2	52.3-124.9
Average diameter of beads ± SD (µm)	121.4 ± 19.4	117.4 ± 18.9	80.9 ± 14.9	78.5 ± 16.8
Estimated water content in beads (v/v)	96.30% *	95.90%	87.48%	86.30%

157 * Data based on a weight measurement previously published (Ashrafi et al., 2017)

158

159 Figure 2 shows optical micrographs of DC Bead *M1* before and after drug loading at different
 160 concentrations. The drug loaded beads remain a spherical shape with no signs of deformation or
 161 fragmentation. The blue colour is due to the presence of the Reactive Blue 4 tint on the bead structure
 162 and the beads loaded with >25 mgmL⁻¹ drug appear more intense in colour as the bead shrinkage
 163 intensifies the appearance of the dye.

164



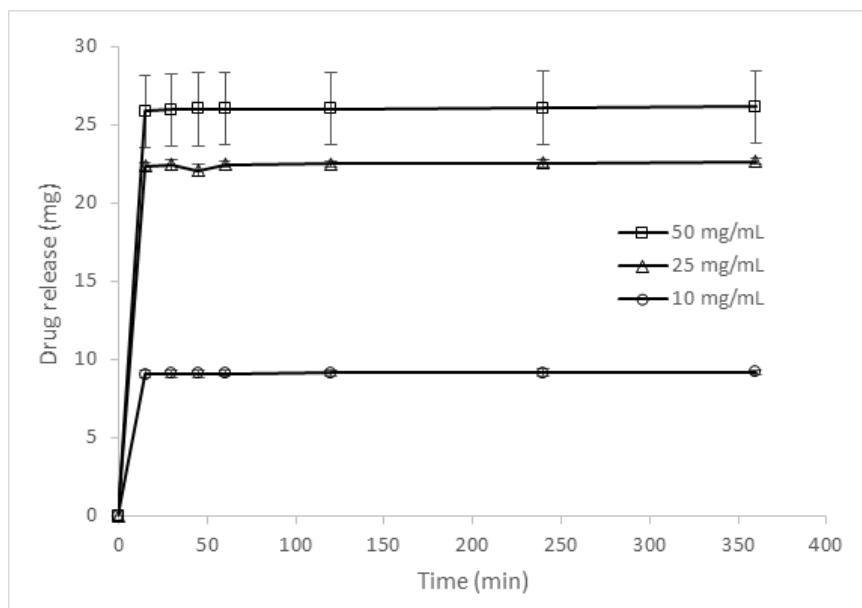
165

166 Figure 2: Microscope images of DC Bead *M1* after loading overnight. A) Bland beads. B) 10
 167 mgmL⁻¹ loading. C) 25 mgmL⁻¹ loading. D) 50 mgmL⁻¹ loading. The scale bar is 500 µm.

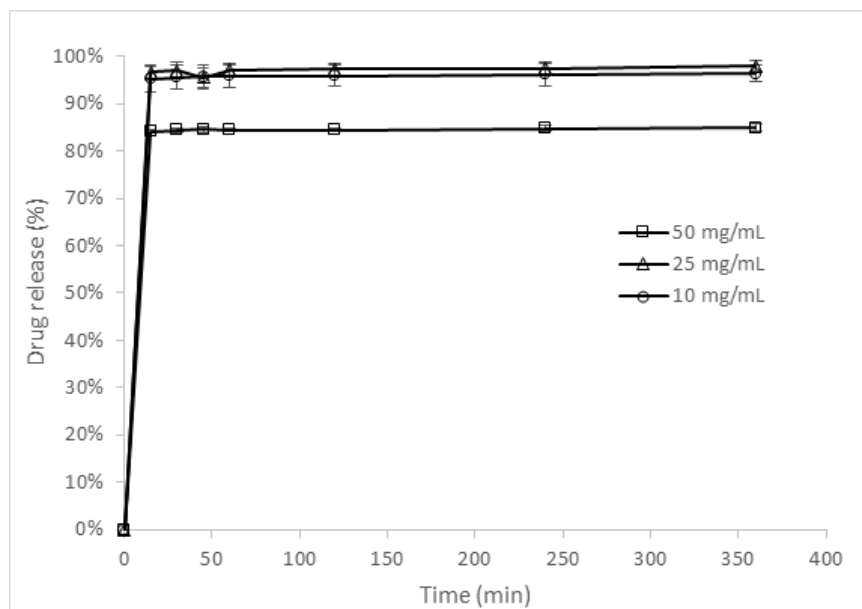
168

169 **Dissolution studies**

170 Three imipramine-based formulations (all containing an equivalent drug content based on drug
171 loading calculations), were analysed to determine the rate and extent of dissolution over a period of
172 360 minutes, as shown in Figure 3.



(A)



(B)

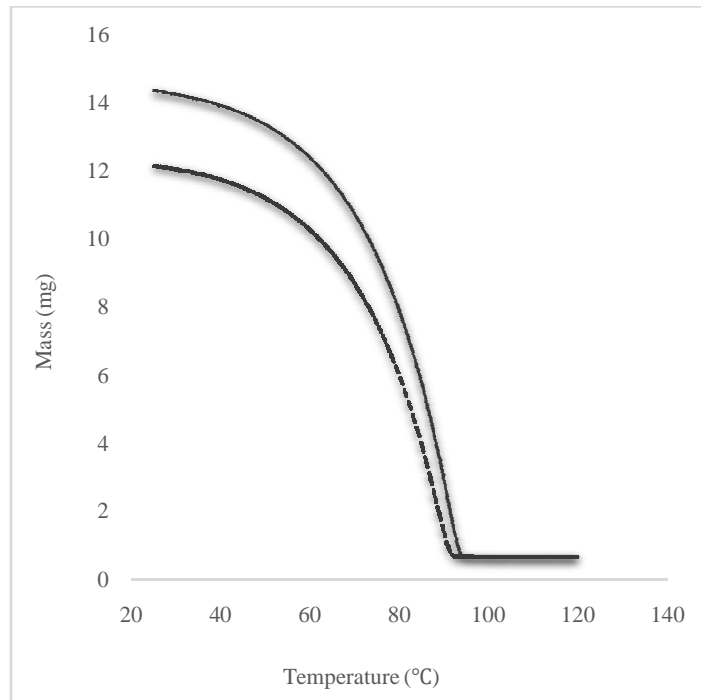
173 Figure 3 Release profiles (amount (A) and percentage release (B)) for beads loaded with 10, 25 and 50
174 mgmL⁻¹ imipramine. Each data point represents the mean of triplicate results (n = 3, ±SD).

175

176 Firstly, drug alone was analysed in this study and it was seen to rapidly undergo dissolution to reach
177 almost 100 % of drug in solution within five minutes (data not shown), this rapid process is partially
178 responsible for the undesirable frequent dosing intervals required for patients with this drug. For the
179 three bead-based formulations analysed it can be clearly seen that the presence of the beads modified
180 the release profiles. Three theoretical drug loadings were considered from 10 to 50 mg/mL with
181 confirmed loading values of 65-99 %, meaning actual loadings of 10, 23 and 31 mgmL⁻¹. Although
182 release is relatively rapid for all formulations, this is not an unusual observation given a USP Type II
183 method was employed that is very efficient at eluting the drug rapidly from the beads. At lower
184 loadings, almost all drug is released within 15 minutes in this test. For the 50mgmL⁻¹ formulation,
185 around 85% of drug is released and with a much slower phase for the remaining 15%. It may be this
186 drug is more tightly bound in the bead structure when loaded at high concentration, suggesting
187 potential drug-drug hydrophobic interactions could be at play (Gonzalez et al., 2008; Lewis et al.,
188 2007) which would account for a much slower second phase of release.

189 **Thermogravimetric analysis(TGA)**

190 TGA was undertaken for three samples of beads with a mass loss of 97.2, 95.6 and 97.5% indicating
191 the beads to contain an average of 3.2 % solid content and 96.8 % water. Previous research has
192 indicated a percentage of water content of 96.3 % using centrifuged mass loss analysis (Ashrafi et al.,
193 2017). This is the first published result using TGA to analyse these type of beads and it is reassuring
194 to see that the values from this work and that published previously are very similar, thus confirming
195 the suitability of TGA as a technique to determine total water content within such beads. Following
196 drug loading, three samples of beads were analysed with a mass loss of 94.6, 95.6 and 96.1 %
197 indicating the beads contained an average of 95.4 % water, i.e. a 1.4 % reduction in water content.
198 This finding correlates well with the results observed regarding bead size in that water content
199 decreased as the beads reduced in size. An example of TGA data obtained for the beads in the absence
200 and presence of drug is shown in Figure 4.



201

202 Figure4:A TGA sample profile for beads alone (solid line) and imipramine with beads (dashed line)
 203 indicating the associated mass loss from water.

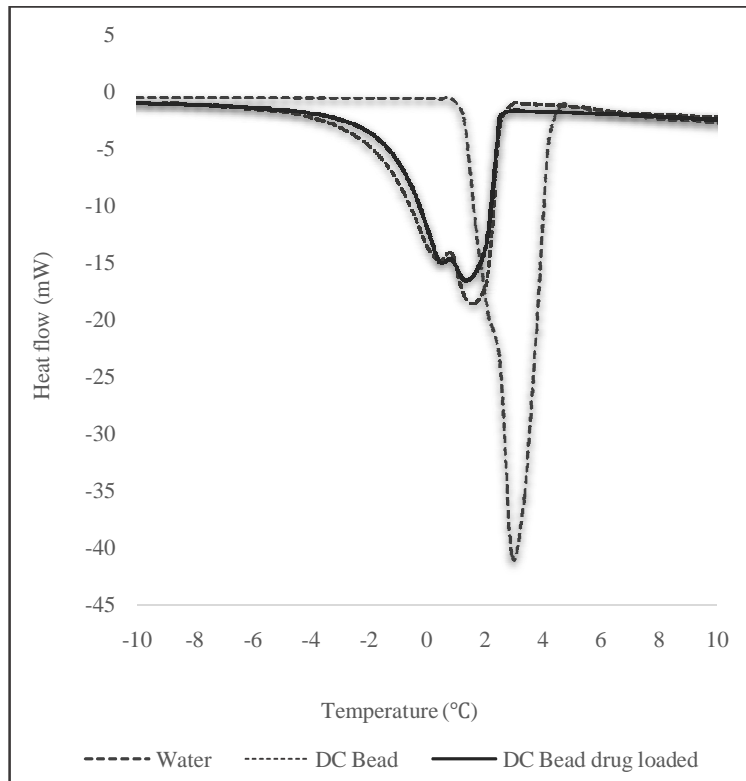
204

205 **Differential scanning calorimetry (DSC)**

206 DSC analysis was completed for the bead samples, both with and without drug present, along with
 207 water to quantify the extent of the water within the beads that could undergo the freezing process.

208 Examples of the data obtained for water alone and a sample of beads are presented in Figure 5.

209



210

211

212 Figure5: DSC profiles for water, DC Bead *M1* and DC Bead *M1* drug loaded.

213

214 Analysis of the data acquired resulted in an average total area for water of $376.8 \pm 9.2 \text{ Jg}^{-1}$ per mg,
 215 $317.3 \pm 0.6.2 \text{ Jg}^{-1}$ per mg for beads without drug (assuming an average water content of 96.8 %) and
 216 $314.1 \pm 9.3 \text{ Jg}^{-1}$ per mg for the beads with drug (assuming an average water content of 95.4 %). As the
 217 error associated with the two bead profiles is greater than the difference between the values it can be
 218 concluded that there was no significant difference in the data, thus implying a similar percentage of
 219 water within the beads was available to undergo the freezing process. However, these values are lower
 220 than that recorded for water alone, thus a proportion of the water within the beads was so tightly
 221 bound that it was unable to freeze (known as non-freezing), as seen in other similar systems
 222 (Hatakeyama and Hatakeyama, 2019; Mlčoch and Kučerík, 2013; Talik and Hubicka, 2018). Through
 223 subtracting the normalised integral for the beads from that of pure water it was possible to calculate
 224 the percentage of non-freezing water present within the beads, with a value for beads alone of 15.8 %
 225 ($\pm 3.2 \%$) and beads with drug of 16.7 % ($\pm 2.9 \%$). These findings indicate that the presence of drug
 226 did not affect the non-freezing water content of the beads with both values being similar within
 227 experimental error. Interestingly, the peaks observed for the beads alone, and with drug, were not
 228 symmetrical, implying that DSC was able to differentiate between the two remaining types of water
 229 within the beads, i.e. that which is loosely bound (known as freezing bound) and the remainder which
 230 is unbound (known as free water). Through deconvolution of the peaks and subsequent integration of

231 the areas it was possible to determine the percentages of the two within the bead. For beads without
232 drug present the 81.0 % water content that was not non-freezing can be further subdivided into 25.1%
233 loosely bound with the remaining 55.9 % unbound. For beads with drug present the 78.7 % water
234 content that was not non-freezing can be further subdivided into 20.5 % loosely bound with the
235 remaining 58.2 % unbound, indicating that the presence of drug more significantly decreased the
236 freezing bound water within the bead rather than the unbound water. This inference is plausible as the
237 unbound water, by its very nature, would be free to be displaced in preference to the partially bound
238 water present.

239

240 **Conclusions**

241 In summary, previous studies had focussed on the application of such beads purely for embolisation
242 purposes, in conjunction with drug delivery. This work presents the first successful incorporation of a
243 drug within the beads, intended for intramuscular or oral drug delivery. Dissolution analysis
244 confirmed the potential of such a system to provide a modified drug release profile, with TGA, DSC
245 and optical microscopy providing an insight into the binding behaviour of water within the beads and
246 how this is affected by the presence of the drug. In conclusion, the results presented in this study
247 confirm the suitability of such beads for a far wider variety of formulation options than those
248 previously adopted and could dramatically expand the usage of such a system for pharmaceutical
249 applications.

250

251 **References**

- 252 Abernethy, D.R., Divoll, M., Greenblatt, D.J., Harmatz, J.S., Shader, R.I., 1984. Absolute bioavailability
253 of imipramine: Influence of food. *Psychopharmacology* 84, 146.
- 254 Abernethy, D.R., Greenblatt, D.J., Shader, R.I., 1985. Imipramine and desipramine disposition in the
255 elderly. *Journal of Pharmacology and Experimental Therapeutics* 232, 183-188.
- 256 Ashrafi, K., Tang, Y., Britton, H., Domenge, O., Blino, D., Bushby, A.J., Shuturminska, K., den Hartog,
257 M., Radaelli, A., Negussie, A.H., Mikhail, A.S., Woods, D.L., Krishnasamy, V., Levy, E.B., Wood,
258 B.J., Willis, S.L., Dreher, M.R., Lewis, A.L., 2017. Characterization of a novel intrinsically
259 radiopaque Drug-eluting Bead for image-guided therapy: DC Bead LUMI™. *Journal of*
260 *Controlled Release* 250, 36-47.
- 261 Boon-in, S., Theerasilp, M., & Crespy, D. (2023). Temperature-Responsive Double-Network Cooling
262 Hydrogels. *ACS Applied Polymer Materials*, 5(4), 2562-2574.
- 263 Budai-Szucs, M., Kiss, E.L., Szilágyi, B.á., Szilágyi, A., Gyarmati, B., Berkó, S., Kovács, A., Horvát, G.,
264 Aigner, Z., Soós, J., Csányi, E., 2018. Mucoadhesive cyclodextrin-modified thiolated
265 poly(aspartic acid) as a potential ophthalmic drug delivery system. *Polymers* 10.
- 266 Caine, M., Zhang, X., Hill, M., Guo, W., Ashrafi, K., Bascal, Z., Kilpatrick, H., Dunn, A., Grey, D., Bushby,
267 R., Bushby, A., Willis, S.L., Dreher, M.R., Lewis, A.L., 2018. Comparison of microsphere
268 penetration with LC Bead LUMI™ versus other commercial microspheres. *Journal of the*
269 *Mechanical Behavior of Biomedical Materials* 78, 46-55.

270 Cai, S., Li, J., Sun, P., Tao, J., Fu, Y., Yang, R., ... & Qu, L. (2023). Red emissive carbon dots-based
 271 polymer beads for recyclable and ultra-sensitive detection of malachite green in fish
 272 tissue. *Sensors and Actuators B: Chemical*, 133311.

273 Dey, M., Das, M., Chowhan, A., Giri, T.K., 2019. Breaking the barricade of oral chemotherapy through
 274 polysaccharide nanocarrier. *International Journal of Biological Macromolecules* 130, 34-49.

275 Gonzalez, M.V., Tang, Y., Phillips, G.J., Lloyd, A.W., Hall, B., Stratford, P.W., Lewis, A.L., 2008.
 276 Doxorubicin eluting beads - 2: Methods for evaluating drug elution and in-vitro:in-vivo
 277 correlation. *Journal of Materials Science: Materials in Medicine* 19, 767-775.

278 Gullapalli, R.P., Mazzitelli, C.L., 2017. Gelatin and Non-Gelatin Capsule Dosage Forms. *Journal of*
 279 *Pharmaceutical Sciences* 106, 1453-1465.

280 Hatakeyama, H., Hatakeyama, T., 2019. Thermal properties of freezing bound water restrained by
 281 sodium lignosulfonate-based polyurethane hydrogels. *Journal of Thermal Analysis and*
 282 *Calorimetry* 135, 2039-2048.

283 Khan, M.S., Roberts, M.S., 2018. Challenges and innovations of drug delivery in older age. *Advanced*
 284 *Drug Delivery Reviews* 135, 3-38.

285 Lewis, A.L., 2009. DC Bead™: A major development in the toolbox for the interventional oncologist.
 286 *Expert Review of Medical Devices* 6, 389-400.

287 Lewis, A.L., Dreher, M.R., O'Byrne, V., Grey, D., Caine, M., Dunn, A., Tang, Y., Hall, B., Fowers, K.D.,
 288 Johnson, C.G., Sharma, K.V., Wood, B.J., 2016. DC BeadM1™: towards an optimal
 289 transcatheter hepatic tumour therapy. *Journal of Materials Science: Materials in Medicine*
 290 27, 1-12.

291 Lewis, A.L., Gonzalez, M.V., Leppard, S.W., Brown, J.E., Stratford, P.W., Phillips, G.J., Lloyd, A.W.,
 292 2007. Doxorubicin eluting beads - 1: Effects of drug loading on bead characteristics and drug
 293 distribution. *Journal of Materials Science: Materials in Medicine* 18, 1691-1699.

294 Lewis, A.L., Gonzalez, M.V., Lloyd, A.W., Hall, B., Tang, Y., Willis, S.L., Leppard, S.W., Wolfenden, L.C.,
 295 Palmer, R.R., Stratford, P.W., 2006. DC Bead: In vitro characterization of a drug-delivery
 296 device for transarterial chemoembolization. *Journal of Vascular and Interventional Radiology*
 297 17, 335-342.

298 Lewis, A.L., Willis, S.L., Dreher, M.R., Tang, Y., Ashrafi, K., Wood, B.J., Levy, E.B., Sharma, K.V.,
 299 Negussie, A.H., Mikhail, A.S., 2018. Bench-to-clinic development of imageable drug-eluting
 300 embolization beads: Finding the balance. *Future Oncology* 14, 2741-2760.

301 Maleki, A., Kettiger, H., Schoubben, A., Rosenholm, J.M., Ambrogi, V., Hamidi, M., 2017. Mesoporous
 302 silica materials: From physico-chemical properties to enhanced dissolution of poorly water-
 303 soluble drugs. *Journal of Controlled Release* 262, 329-347.

304 Manna, S., Wu, Y., Wang, Y., Koo, B., Chen, L., Petrochenko, P., Dong, Y., Choi, S., Kozak, D., Oktem,
 305 B., Xu, X., Zheng, J., 2019. Probing the mechanism of bupivacaine drug release from
 306 multivesicular liposomes. *Journal of Controlled Release* 294, 279-287.

307 Mlčoch, T., Kučerík, J., 2013. Hydration and drying of various polysaccharides studied using DSC.
 308 *Journal of Thermal Analysis and Calorimetry* 113, 1177-1185.

309 Smith, O. E., Waters, L. J., Small, W., & Mellor, S. (2022). CMC determination using isothermal
 310 titration calorimetry for five industrially significant non-ionic surfactants. *Colloids and*
 311 *Surfaces B: Biointerfaces*, 211, 112320

312 Ramey, K., Ma, J.D., Best, B.M., Atayee, R.S., Morello, C.M., 2014. Variability in metabolism of
 313 imipramine and desipramine using urinary excretion data. *Journal of Analytical Toxicology*
 314 38, 368-374.

315 Swaine, T.S., Garcia, P., Tang, Y., Lewis, A.L., Parkes, G., Waters, L.J., 2019. Characterizing Drug-
 316 Polymer Bead Interactions Using Isothermal Titration Calorimetry. *Journal of Pharmaceutical*
 317 *Sciences*.

318 Talik, P., Hubicka, U., 2018. The DSC approach to study non-freezing water contents of hydrated
 319 hydroxypropylcellulose (HPC): A study over effects of viscosity and drug addition. *Journal of*
 320 *Thermal Analysis and Calorimetry* 132, 445-451.

- 321 Taylor, R.R., Tang, Y., Gonzalez, M.V., Stratford, P.W., Lewis, A.L., 2007. Irinotecan drug eluting beads
322 for use in chemoembolization: In vitro and in vivo evaluation of drug release properties.
323 European Journal of Pharmaceutical Sciences 30, 7-14.
- 324 Ullmann, U., Lehnfeld, R., Bliesath, H., Birkel, M., Gebbing, H., Gräve, M., Wolf, H., 2001. Relative
325 bioavailability of imipramine (Tofranil) coated tablets in healthy volunteers. International
326 Journal of Clinical Pharmacology and Therapeutics 39, 271-276.
- 327 Waters, Swaine, T.S., Lewis, A.L., 2015. A calorimetric investigation of doxorubicin-polymer bead
328 interactions. International Journal of Pharmaceutics 493, 129-133.
- 329 Waters, L.J., Hanrahan, J.P., Tobin, J.M., Finch, C.V., Parkes, G.M.B., Ahmad, S.A., Mohammad, F.,
330 Saleem, M., 2018. Enhancing the dissolution of phenylbutazone using Syloid® based
331 mesoporous silicas for oral equine applications. Journal of Pharmaceutical Analysis 8, 181-
332 186.
- 333 Wersig, T., Krombholz, R., Janich, C., Meister, A., Kressler, J., Mäder, K., 2018. Indomethacin
334 functionalised poly(glycerol adipate) nanospheres as promising candidates for modified drug
335 release. European Journal of Pharmaceutical Sciences 123, 350-361.
- 336 Xie, H., Zong, Y., Chen, Y., Hu, D., Xu, Z., & Zhao, L. (2023). Numerical investigation on
337 preparation of expanded polymer beads using supercritical CO₂ in a spouted bed. *Chemical*
338 *Engineering Science*, 267, 118331.
- 339